



You have downloaded a document from
RE-BUS
repository of the University of Silesia in Katowice

Title: Characteristic of carbon nanotubes modified with cobalt, copper and bromine

Author: P. Zygoń, Jerzy Peszke, M. Gwozdzik, Z. Nitkiewicz, M. Malik

Citation style: Zygoń P., Peszke Jerzy, Gwozdzik M., Nitkiewicz Z., Malik M. (2014). Characteristic of carbon nanotubes modified with cobalt, copper and bromine. "Archives of Metallurgy and Materials" (2014, iss. 2, s. 675-679), doi 10.2478/amm-2014-0110



Uznanie autorstwa - Użycie niekomercyjne - Bez utworów zależnych Polska - Licencja ta zezwala na rozpowszechnianie, przedstawianie i wykonywanie utworu jedynie w celach niekomercyjnych oraz pod warunkiem zachowania go w oryginalnej postaci (nie tworzenia utworów zależnych).



UNIwersYTET ŚLĄSKI
W KATOWICACH



Biblioteka
Uniwersytetu Śląskiego



Ministerstwo Nauki
i Szkolnictwa Wyższego

P. ZYGOŃ*, J. PESZKE**, M. GWOŹDZIK*, Z. NITKIEWICZ*, M. MALIK***

CHARACTERISTIC OF CARBON NANOTUBES MODIFIED WITH COBALT, COPPER AND BROMINE

CHARAKTERYSTYKA NANORUREK WĘGLOWYCH MODYFIKOWANYCH KOBALTEM, MIEDZIĄ I BROMEM

The paper presents results of studies on carbon nanotubes – as received, after cleaning and also after modification. Functional groups as well as metal nanoparticles have been attached, originating from cobalt sulphate, copper acetate and a mixture of hydrogen bromide and bromide. The surface studies on an atomic forces microscope (AFM), X-ray studies (phase composition analysis, crystallite sizes determination) as well as Raman spectroscopy studies were carried out on such nanotubes.

The surface topography studies have shown that after the modification the diameter and length of nanotubes change. Also the surface development changes, which has been determined through roughness parameter measurements.

The change of intensity, of crystallite size and of half-value width of main reflections originating from carbon for nanotubes modified in various ways have been determined using the X-ray analysis.

Keywords: carbon nanotubes, AFM, Raman spectrum, modification

W pracy przedstawiono wyniki badań nanorurek węglowych w stanie surowym, po oczyszczeniu jak również po modyfikacji. Zostały przyłączone grupy funkcyjne oraz nanocząstki metali, pochodzące od siarczynu kobaltu, octanu miedzi i mieszaniny bromowodoru z bromem. Dla takich nanorurek przeprowadzono badania powierzchni na mikroskopie sił atomowych (AFM), badania rentgenograficzne (analiza składu fazowego, określenie wielkości kryształitów) oraz badania spektroskopowe Ramana.

Badania topografii powierzchni wykazały, że po modyfikacji nanorurek zmienia się ich średnica i długość. Zmienia się również rozwinięcie powierzchni co zostało wyznaczone za pomocą określenia parametru chropowatości.

Za pomocą analizy rentgenograficznej określono zmianę intensywności, wielkości kryształitów oraz szerokości połówkowej refleksów głównych pochodzących od węgla dla nanorurek różnie modyfikowanych.

1. Introduction

A great interest in carbon nanotubes (CNTs) started in 1991, when the S. Iijima paper on cylindrical nanometric sp^2 type carbon structures was published. CNTs belong to the group of so-called nanomaterials, which feature unique physical properties, resulting directly from their structure of nanometric dimensions [1, 2].

They are constructed of a single ring (single wall carbon nanotubes, SWCNT) or of a few (multiwall carbon nanotubes, MWCNT) concentric and coaxial cylinders, which are rolled single graphite planes, named graphene planes [3]. Two types of nanotubes – chiral and non-chiral [4] are distinguished depending on the way of graphite plane rolling. The chiral nature of a nanotube has a significant impact on its properties, especially the electrical properties [5].

Carbon nanotubes feature a low density of $\sim 2.1 \text{ g/cm}^3$ and a highly developed specific surface area. They have a high tensile strength up to 500 GPa, the elastic modulus reaches 7-8 TPa and they feature a high resistance to high temperatures ($>3000^\circ\text{C}$ in vacuum) [6]. They superbly conduct the electric

current and it is anticipated that they can withstand the current density of 1 GA/cm^2 , which combined with their small diameters makes that they are a perfect material to create paths in electronic circuits [7]. At a small diameter (1-80 nm) and a high aspect ratio (L/D even above 10,000) they are potentially an attractive reinforcing material for polymers, ceramic materials and metals [8]. The composites obtained with the use of nanotubes have not only a good mechanical strength and electric conduction but also are easily machinable without origination of cracks, which occur on carbon fibres [9].

To improve their unique properties the CNTs are subject to chemical modifications. The attachment of functional groups to nanotubes may have a huge impact on their properties, e.g. solubility in solvents or polymer matrices.

2. Material and experimental methods

CNT CO. LTD carbon nanotubes, with a commercial name $C_{TUBE} 100$, obtained using the thermal CVD method, were used as the studied material. Raw nanotubes were 1 to

* CZESTOCHOWA UNIVERSITY OF TECHNOLOGY, INSTITUTE OF MATERIALS ENGINEERING, 19 ARMII KRAJOWEJ AV., 42-201 CZĘSTOCHOWA, POLAND

** UNIVERSITY OF SILESIA IN KATOWICE, DEPARTMENT OF SOLID STATE PHYSICS, ST. UNIWERSYTECKA 4, 40-007 KATOWICE, POLAND

*** CZESTOCHOWA UNIVERSITY OF TECHNOLOGY, DEPARTMENT OF CHEMISTRY, 19 ARMII KRAJOWEJ AV., 42-201 CZĘSTOCHOWA, POLAND

25 μm long, 10 to 40 nm in diameter, with the density of 0.03 – 0.06 g/cm^3 and the specific surface area of 150 – 250 m^2/g . Before the studies the carbon nanotubes were subject to cleaning to remove the pollution originating from amorphous carbon, carbon black and catalyst particles. The CNTs cleaning was carried out using a liquid phase and consisted in treating the as-received material with oxidising liquids (a mixture of concentrated nitric acid (HNO_3) and concentrated sulphuric acid (H_2SO_4)) at the boiling point. The flask containing carbon nanotubes and the mixture of nitric and sulphuric acids, at the ratio of 3:1, was subject to the action of ultrasounds during 1 hour to break agglomerates. Then the flask was heated and maintained at the boiling point during approx. 10 hours. During the cleaning the amorphous carbon is much faster oxidised and degraded than the undefected CNT structures. Also catalysts and their carriers are removed in this process. Defects favourable to the formation of chemical groups, including the carboxyl groups, are formed in the structure during the nanotubes cleaning.

The formed carboxylated nanotubes were treated with ammonia to obtain ammonia groups (CNT-COONH_4) on the CNTs surface. CNT-COONH_4 were then modified with copper and cobalt particles. The copper particles originated from the copper acetate and the cobalt particles from the cobalt sulphate. The proportion of nanotubes to a pure metal, used during the modification, was approx. 2:1. The carboxylated carbon nanotubes were subject to the action of bromide and hydrobromic acid mixture to enrich their surface with bromide particles. Initially there was a reaction of NH_4^+ ions replacement with metal ions and then the whole was reduced using the ascorbic acid. As a result, metal particles were formed on the salt surface, being the reaction precursors.

The ammonified carboxylated nanotubes, with copper, cobalt and bromide particles on the surface, were then subject to the following studies:

- surface topography studies,
- X-ray studies,
- Raman spectroscopy studies.

Studies of surface topography were performed on a VEECO MULTIMODE atomic forces microscope (AFM) with a NANOSCOPE controller by means of the Tapping Mode method, acquiring the data on the height and on the phase imaging. Powders for the research have been applied to a conductive pad. The surface studies were carried out in the area of $1\ \mu\text{m} \times 1\ \mu\text{m}$.

The X-ray phase analysis was carried out using a SEIFERT 3003T/T X-ray diffractometer with a cobalt tube of $\lambda = 0.17902\ \text{nm}$ wavelength. The X-ray studies were performed comprising measurements at a symmetric Bragg-Brentano geometry (XRD) within the $20\text{--}120^\circ$ range of angles with an angular step of 0.1° and the exposure time of 3 seconds. To interpret the results (to determine the 2θ position and the total intensity I_{Net} and the crystallite sizes) the diffractograms were described by a Pseudo Voigt curve using the Analyze software. According to the crystallographic database DHN PDS with catalog number 25-0284 angle 2θ for coal is 31.01 . Based on the half-value width and the position of main carbon reflections the crystallites size was determined using the Scherrer formula [10, 11, 12] (1):

$$D_{hkl} = \frac{K \cdot \lambda}{\beta \cdot \cos \theta} \quad (1)$$

where:

D_{hkl} – mean crystallite size in the direction normal to the specimen surface,

K – Scherrer constant,

λ – radiation wavelength, nm

β – reflection half-value width, rad

θ – Bragg angle

A computer software and the DHN PDS crystallographic database were used for the phase identification.

The Raman spectroscopy studies were performed on a Raman spectrometer EnWAVE OPTRONICS type EZRaman-L coupled with an optical microscope. The studies were carried in the area up to $2400\ \text{cm}^{-1}$. The Raman spectroscopy provides information on the atomic bonds, the crystal structure and nanocrystalline and amorphous carbon systems.

3. Results of Tests

During the test on AFM, were performed 5 scans for each sample. Sample images are presented in Fig. 1-5. Figure 1a presents the image of carboxylated nanotubes (cleaned in a mixture of concentrated nitric and sulphuric acids) obtained during studies on an atomic forces microscope (AFM). The nanotubes diameter is diversified and ranges from a few to tens nanometres. Nanotubes differ in length and are bent in various directions. However, it is possible to notice places of low degree of entanglement (agglomerations).

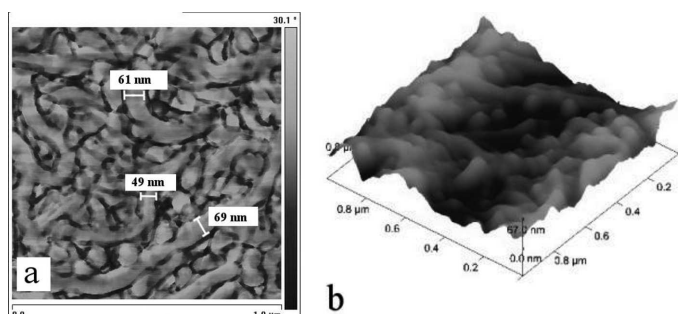


Fig. 1. Surface of carboxylated nanotubes: a) 2D image (AFM); b) 3D image (AFM)

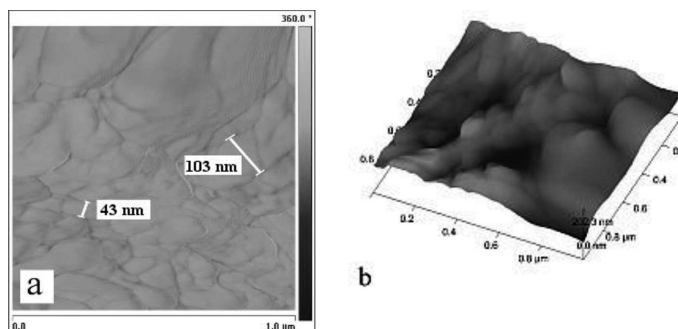


Fig. 2. Surface of ammonified nanotubes: a) 2D image (AFM); b) 3D image (AFM)

The surface topography has shown that the ammonified carbon nanotubes feature a pretty specific appearance

(Fig. 2). From the phase imaging (Fig. 1a) we can see that the CNT-COONH₄ resemble panels and are quite defected. The panels diameter ranges from a few to as many as a few dozen nanometres.

Fig. 3 shows the image of ammonified nanotubes with cobalt particles on the surface. The diameter of nanotubes modified this way ranges between 40 and 70 nm. It is noticeable that they are a bit shorter than the initial material, which consisted of carboxylated carbon nanotubes. A banded arrangement of carbon nanotubes is visible on the 2D surface.

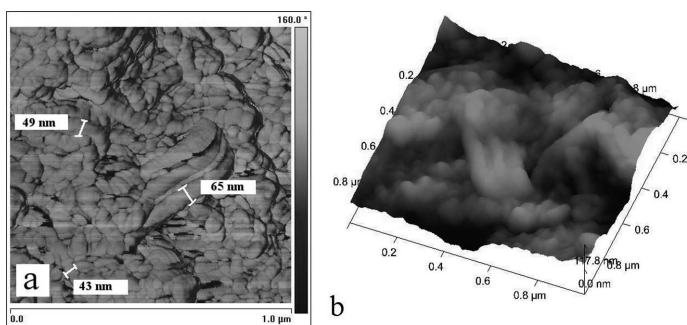


Fig. 3. Surface of ammonified nanotubes with cobalt particles: a) 2D image (AFM); b) 3D image (AFM)

The surface of carbon nanotubes with copper particles on the surface is presented in Fig. 4. Very entangled and compact nanotubes are visible on the 2D surface. Their appearance does not remind long tubes but rather more flat and compact structures. Evenly distributed nanotube panels are noticeable on the 3D image.

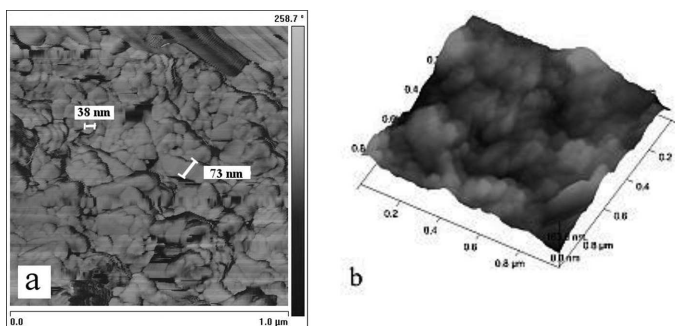


Fig. 4. Surface of ammonified nanotubes with copper particles: a) 2D image (AFM); b) 3D image (AFM)

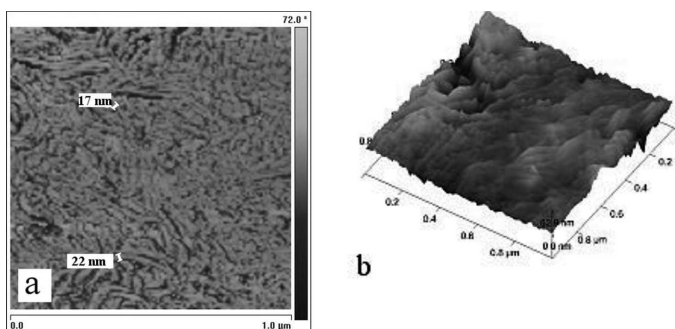


Fig. 5. Surface of carboxylated nanotubes modified with bromide: a) 2D image (AFM); b) 3D image (AFM)

Fig. 5 presents the surface of carboxylated carbon nanotubes with bromide particles. Fig. 5a shows many pretty long

threads, albeit small in diameter, because only ~20 nm. The 3D surface (Fig. 5b) reveals that the nanotubes are arranged linearly, which proves a good breaking of agglomerates.

The obtained roughness parameters R_a are presented in Fig. 6. A lower roughness of carboxylated nanotubes is caused by the fact that the nanotubes cleaned in sulphuric and nitric acids form smooth shapes with a metallic lustre. The ammonified nanotubes and the copper- and cobalt-modified ammonified nanotubes show very close roughness parameters. However, the non-modified ammonified nanotubes feature a slightly higher roughness equal to 22.3 nm, for the copper-modified nanotubes it is 19.3 nm, while for the cobalt-modified ammonified nanotubes the roughness is lower, equal to 17.3 nm. The carboxylated nanotubes enriched with bromide feature the lowest roughness. Their roughness is equal to 7.1 nm. Standard deviation of the R_a is equal 0.7 nm and for the R_{max} is equal 4 nm.

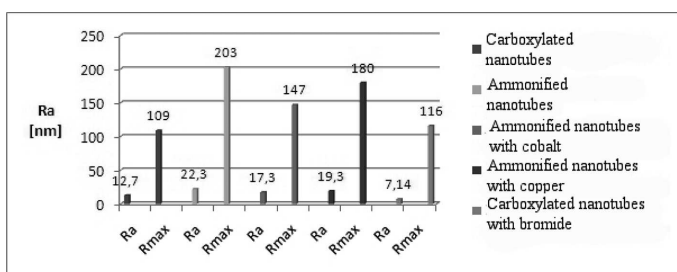


Fig. 6. Roughness parameters for individual carbon nanotubes

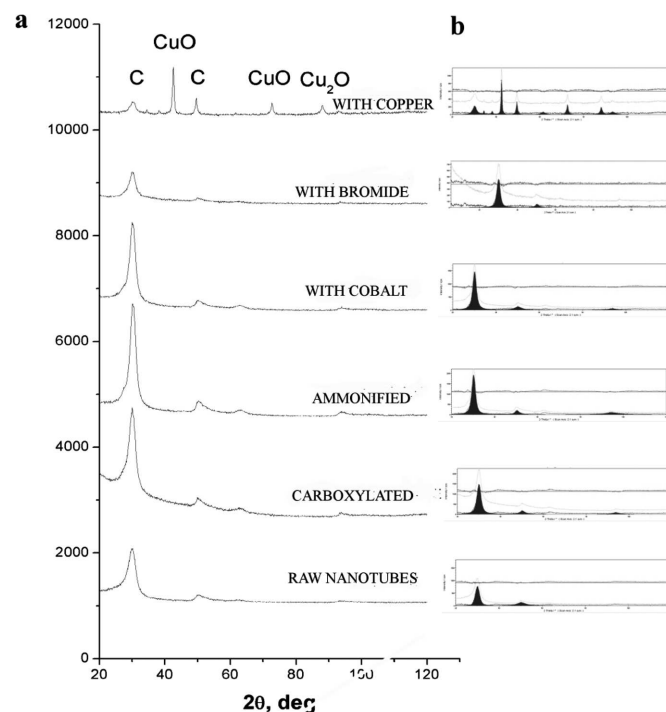


Fig. 7. The X-ray diffractograms of as received and modified nanotubes (a); fitting by means of the Analyze software (b)

The results of X-ray studies of carbon nanotubes after cleaning and after their surface modification with nanoparticles of copper, cobalt and bromide originating from the copper acetate, cobalt sulphate and a mixture of bromide with hydrogen bromide, respectively, are presented in Fig. 7. The X-ray

phase analysis has shown that characteristic reflections originating from carbon are visible on the diffractograms. Peaks originating from copper oxides are also noticeable in the nanotubes modified with copper particles. The main reflections originating from carbon were subject to a more thorough analysis (Fig. 8).

The total intensity of reflections originating from carbon is the highest for carboxylated and ammonified nanotubes and the lowest for bromide- and copper-modified nanotubes (Fig. 8).

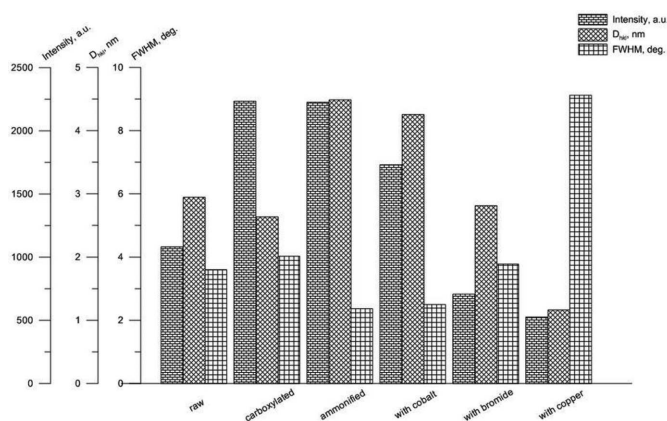


Fig. 8. Total intensity and half-value width and D_{hkl} crystallite sizes of the main reflection originating from carbon vs. the type of nanotubes

The narrowest diffraction line was observed for ammonified nanotubes and nanotubes enriched with bromide. Instead, the widest for copper-modified nanotubes, which is caused by the decrease in the crystallites size. X-ray studies performed on nanotubes modified in various ways show that it is not only the intensity, which changes, but also the half-value width of reflections. As it is known a change of the width can result from both the crystallite size and from stresses in the material. The D_{hkl} crystallite size determined from the Scherrer formula (1) changes depending on the modification type.

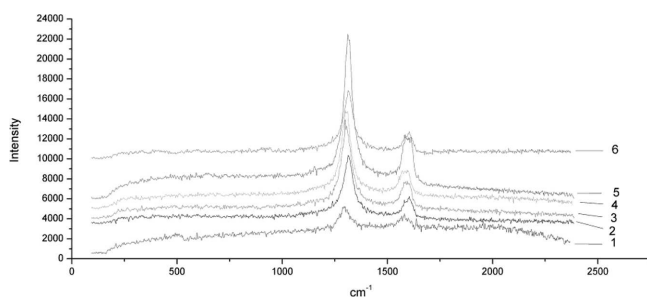


Fig. 9. Raman spectrum of as received complex nanotubes (1) together with the spectrum of ammonified nanotubes (2) and with the spectrum of nanotubes enriched with bromide particles (3) and with the spectrum of nanotubes enriched with cobalt particles (4) and with the spectrum of carboxylated nanotubes (5) and with the spectrum of nanotubes enriched with copper particles (6)

Figures 9 present the results of Raman studies. For majority of carbon coatings the Raman spectrum is dominated by two bands situated in the area $\sim 1500 \text{ cm}^{-1}$. They may be decomposed into two lines situated around 1350 cm^{-1} and 1550 cm^{-1} . The peak around 1350 cm^{-1} occurs during the growth of an unordered graphite structure. It results from the

occurrence of annular space configuration of carbon bonds of sp^2 hybridisation [13]; also sp^1 and sp^3 bonds are formed then. Instead, the peak around 1550 cm^{-1} is active in a monocrystalline graphite and originates from a chain spatial configuration of carbon bonds of sp^2 hybridisation. An increase in the peak around 1350 cm^{-1} intensity as against the peak around 1550 cm^{-1} indicates a growth of the existing aromatic rings or the formation of new ones.

4. Summary of results

Before the application in further modifications and studies the carbon nanotubes were subject to cleaning. The cleaning was carried out in a liquid phase in a mixture of concentrated oxidising acids: nitric and sulphuric. The cleaning is carried out to obtain better properties of nanotubes and also to obtain proper results of the scientific research on those structures, because the presence of metallic nanoparticles (Fe, Ni, etc.) may distort the research results.

The studies of carbon nanotubes surface topography before and after the modification have shown that the surface of ammonified nanotubes is the most developed, which is proven by the Ra parameter. For the ammonified nanotubes the Ra parameter is equal to $\sim 22.3 \text{ nm}$, while carbon nanotubes enriched with bromide particles feature the least developed surface. For them the Ra parameter is equal to $\sim 7.4 \text{ nm}$. The surface topography studies have also shown that after the process of cleaning and modifying both the diameter and the length of the initial material decrease.

The X-ray analysis has shown that crystallites originating from the main reflection of carbon are the largest for ammonified nanotubes and for nanotubes enriched with cobalt particles and at the same time the diffraction lines for such nanotubes are narrowed. Instead, the nanotubes enriched with copper and bromide particles show the lowest value and the widest diffraction line, which depends on the crystallites size.

Characteristic reflections are visible on the Raman spectra, occurring around 1500 cm^{-1} , which originate from carbon, mainly of sp^2 hybridisation. A greater peak intensity in the area $\sim 1350 \text{ cm}^{-1}$ as compared with the peak intensity around 1550 cm^{-1} indicates the growth of aromatic rings and the formation of new ones.

REFERENCES

- [1] W. Królikowski, Z. Rosłaniec, *Kompozyty* **9**, 3-15 (2004).
- [2] G. Zhu, X.P. Zhou, J. Cheng, M.F. Wang, Y. Su, *Arch. Metall. Mater.* **53**, 3, 735-740 (2008).
- [3] P. Zygón, J. Peszke, XIII International Scientific Conference. New technologies and achievements in metallurgy and materials engineering **24**, 740-743 (2012).
- [4] A. Huczko, *Nanorurki węglowe. Czarne diamenty XXI wieku*, (2004).
- [5] Ł. Pietrzak, J.K. Jeszka, *Polimery* **55**, 7-8, 524-528 (2010).
- [6] B.I. Yakobson, *Chem. Int. Ed.* **41**, 1853-1859 (2002).
- [7] W. Przygodzki, A. Włochowicz, *Fulereny i nanorurki*, WNT (2001).

- [8] Z. Rosłaniec, Zeszyty Naukowe Politechniki Poznańskiej **4**, 211-215 (2007).
- [9] M. Bystrzejewski, T. Pichler, M. Ruemmeli, Wiadomości Chemiczne Z. **60**, 9-10, 569-607 (2006).
- [10] M. Gwoździk, Z. Nitkiewicz, Arch. Metall. Mater. **58**, 1, 31-34 (2013).
- [11] D. Oleszak, A. Olszyna, Kompozyty **4**, 284-288 (2004).
- [12] A. Malek, B. Projjal, Journal of Alloys and Compounds **491**, 582-583 (2010).
- [13] A.C. Ferrari, J. Robertson, Phys. Rev. B **61**, 14096-14107 (2000).

Received: 10 September 2013.